

# From Node Interaction to Hop Interaction: New Effective and Scalable Graph Learning Paradigm

Jie Chen<sup>1</sup>, Zilong Li<sup>1</sup>, Yin Zhu<sup>1</sup>, Junping Zhang<sup>1</sup>, Jian Pu<sup>2</sup>

<sup>1</sup>Shanghai Key Lab of Intelligent Information Processing, School of Computer Science, Fudan University, China

<sup>2</sup>Institute of Science and Technology for Brain-Inspired Intelligence, Fudan University, China

chenj19@fudan.edu.cn, zilongli21@m.fudan.edu.cn, yinzhu20@fudan.edu.cn,

jpzhang@fudan.edu.cn, jianpu@fudan.edu.cn

## ABSTRACT

Existing Graph Neural Networks (GNNs) follow the message-passing mechanism that conducts information interaction among nodes iteratively. While considerable progress has been made, such node interaction paradigms still have the following limitation. First, the scalability limitation precludes the wide application of GNNs in large-scale industrial settings since the node interaction among rapidly expanding neighbors incurs high computation and memory costs. Second, the over-smoothing problem restricts the discrimination ability of nodes, i.e., node representations of different classes will converge to indistinguishable after repeated node interactions. In this work, we propose a novel hop interaction paradigm to address these limitations simultaneously. The core idea of hop interaction is to convert the target of message-passing from nodes into multi-hop features inside each node. Specifically, it first pre-computed multi-hop features of nodes to reduce computation costs during training and inference. Then, it conducts a non-linear interaction among multi-hop features to enhance the discrimination of nodes. We design a simple yet effective HopGNN framework that can easily utilize existing GNNs to achieve hop interaction. Furthermore, we propose a multi-task learning strategy with a self-supervised learning objective to enhance HopGNN. We conduct extensive experiments on 12 benchmark datasets in a wide range of domains, scales, and smoothness of graphs. Experimental results show that our methods achieve superior performance while maintaining high scalability and efficiency.

## KEYWORDS

Graph Neural Networks, Representation Learning, Over-smoothing, Scalability

## ACM Reference Format:

Jie Chen<sup>1</sup>, Zilong Li<sup>1</sup>, Yin Zhu<sup>1</sup>, Junping Zhang<sup>1</sup>, Jian Pu<sup>2</sup>. 2018. From Node Interaction to Hop Interaction: New Effective and Scalable Graph Learning Paradigm. In *Proceedings of Make sure to enter the correct conference title from your rights confirmation email (Conference acronym 'XX)*. ACM, New York, NY, USA, 11 pages. <https://doi.org/XXXXXXX.XXXXXXX>

Permission to make digital or hard copies of all or part of this work for personal or classroom use is granted without fee provided that copies are not made or distributed for profit or commercial advantage and that copies bear this notice and the full citation on the first page. Copyrights for components of this work owned by others than ACM must be honored. Abstracting with credit is permitted. To copy otherwise, or republish, to post on servers or to redistribute to lists, requires prior specific permission and/or a fee. Request permissions from [permissions@acm.org](mailto:permissions@acm.org).

Conference acronym 'XX, June 03–05, 2018, Woodstock, NY

© 2018 Association for Computing Machinery.

ACM ISBN 978-x-xxxx-xxxx-x/YY/MM...\$15.00

<https://doi.org/XXXXXXX.XXXXXXX>

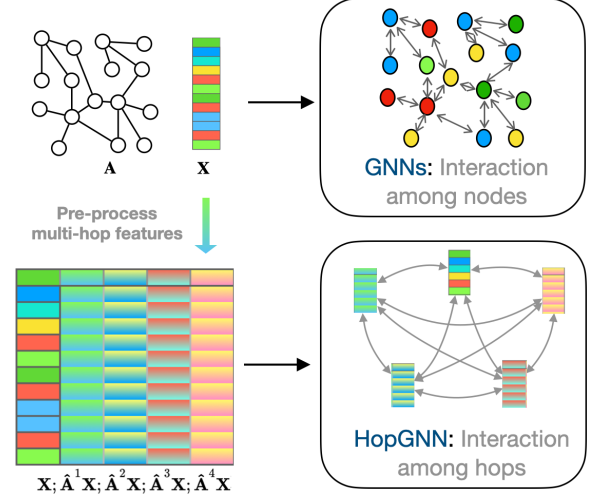


**Figure 1: Comparison of node interaction and hop interaction. The hop interaction first pre-computes multi-hop features and then conducts non-linear interaction among different hops via GNNs, which enjoy high efficiency and effectiveness.**

## 1 INTRODUCTION

Graph Neural Networks (GNNs) have recently become very popular for graph machine learning research and have demonstrated great results on a wide range of graph applications, including social networks [33], point cloud analysis [32] and recommendation systems [17]. The core success of GNNs lies in the message-passing mechanism that iteratively conducts information interaction among nodes [14]. Each node in a graph convolution layer first aggregates information from local neighbors and combines them with non-linear transformation to update the self-representation. After stacking  $K$  layers, nodes can be aware of long-range  $K$ -hop neighbor information and obtain representative representations for downstream tasks [24, 39]. However, despite the success of such popular node interaction paradigms in GNNs, the number of neighbors for each node would grow exponentially with layers [2], which results in the well-known *scalability* and *over-smoothing* limitation of GNNs.

The *scalability* limitation precludes the broad application of GNNs in large-scale industrial settings since the node interaction among rapidly expanding neighbors incurs high computation and memory costs [45]. Although we can reduce the size of neighbors by sampling techniques [5, 16], it still executes node interaction iteratively during training, and the performance is highly sensitive

to the sampling quality [12]. Recently, scalable GNNs that focus on simplifying or decoupling node interactions have emerged [38, 47]. Such decoupled GNNs first pre-compute the linear aggregation of  $K$ -hop neighbors to generate node features and then utilize the MLP to each node without considering the graph structure during training and inference. However, despite high efficiency and scalability, such methods lead to suboptimal results due to the lack of nonlinear interactions between nodes.

Another limitation is *over-smoothing*, which restricts the discrimination ability of nodes, *i.e.*, node representations of different classes will converge to indistinguishable after repeated node interactions [26]. On the one hand, it causes the performance of GNNs to degenerate when increasing the layers [22, 28]. On the other hand, recent work has also found that even the shallow GNNs are surprisingly inferior to MLP on some heterophily datasets [31]. Since the connected nodes on heterophily datasets are usually from different classes, the massive local inter-class neighbors would still cause node interaction to blur the class boundaries [48]. Recently, to consider the neighbor influence of each hop for maintaining the node discrimination, emerging advanced node interaction GNNs, such as deep GNNs with residual connection [8, 24] and heterophilic-graph-oriented GNNs with adaptive aggregation [4, 34, 48], have achieved promising results. However, although adaptively considering the influence of each hop neighbor, they still suffer from high computational costs and cannot handle large-scale datasets.

These two limitations have mostly been studied independently. Resolving one side usually comes at the expense of the other. However, can we bridge the two worlds, enjoying the low-latency, node-interaction-free decoupled GNNs and the high discrimination ability of advanced node interaction GNNs simultaneously? We argue that it is possible to convert the node interaction into a hop interaction paradigm without losing performance, but drastically reducing the computational cost. As shown in Figure 1, the core idea of hop interaction is to decouple the whole node interaction into two parts, the non-parameter hop feature pre-processing and non-linear interaction among hops. Inspired by the recommendation system, the non-linear interaction among different semantic features can enhance discrimination [15], *e.g.*, model the co-occurrence of career, sex and age of a user to identify its interest. We can treat the pre-compute  $L$  hops neighbor as  $L$  semantic features of each node and regard the node classification as a feature interaction problem, *i.e.*, model the non-linear hop interaction to obtain a discriminative representation of each node.

To this end, we design a simple yet effective HopGNN framework to address the above limitation simultaneously. It first pre-computes the multi-hop representation according to the graph structure. Then, to enhance the discriminative ability without node interaction, we can construct a hop feature graph over each node and utilize GNNs on the graph to achieve hop interaction in a flexible and explicit fashion. Without loss of generality, we implement an attention-based interaction HopGNN layer and average pooling to fuse multi-hop features and generate the final prediction. Furthermore, to show the generality and flexibility of our framework, we provide a multi-task learning strategy that combines the self-supervised objective to enhance performance.

Our contributions are summarized as follows:

1. *New perspective*: We propose a new graph learning paradigm that goes from node interaction to hop interaction. It aims at first non-parameter precomputing over the multi-hop neighbor features and then conducting non-linear interaction among them.

2. *General and flexible framework*: We design a simple yet effective HopGNN framework for hop interaction. Besides, the HopGNN is general and flexible to combine the self-supervised objective to easily enhance performance.

3. *State-of-the-art performance*: The experimental results demonstrate that HopGNN achieves state-of-the-art performance on 12 graph datasets of diverse domains, sizes and graph heterophilies while maintaining high scalability and efficiency.

## 2 BACKGROUND AND RELATED WORKS

### 2.1 Notation and Node Classification

Consider a graph  $\mathcal{G} = (\mathcal{V}, \mathcal{E})$ , with  $N$  nodes and  $E$  edges. Let  $\mathbf{A} \in \mathbb{R}^{N \times N}$  be the adjacency matrix, with  $\mathbf{A}_{i,j} = 1$  if  $\text{edge}(i, j) \in \mathcal{E}$ , and 0 otherwise. The features of nodes are formed by  $\mathbf{X} \in \mathbb{R}^{N \times d}$ , and the labels are represented by  $\mathbf{Y} \in \mathbb{R}^{N \times c}$ . Given a set of labeled nodes  $\mathcal{V}_{\mathcal{L}}$ , the task of node classification is to predict the labels of the unlabeled nodes  $\mathcal{V}_{\mathcal{U}}$  by exploiting the graph adjacency matrix  $\mathbf{A}$  and the features  $\mathbf{X}$ .

Besides, the notion of homophily and heterophily corresponds to the smoothness of the signal  $\mathbf{Y}$  on the graph  $\mathcal{G}$ . The edge homophily ratio of the graph is defined as  $\mathcal{H}_{\text{edge}} = \frac{|\{(u,v) \in \mathcal{E} \wedge y_u = y_v\}|}{|\mathcal{E}|}$ , while  $\mathcal{H}_{\text{edge}}$  tends to 1 means high homophily and low heterophily, and vice versa.

### 2.2 Graph Neural Networks

**Standard node interaction GNNs.** Each layer of most node interaction GNNs follows the message-passing mechanism [14] that is composed of two steps: (1) aggregate information from neighbors:  $\mathbf{m}_i^l = \text{AGGREGATE}(\mathbf{h}_j^l, v_j \in \mathcal{N}_i)$ ; (2) update representation:  $\mathbf{h}_i^{l+1} = \text{UPDATE}(\mathbf{h}_i^l, \mathbf{m}_i^l)$ . To capture long-range neighbor information, standard node interaction GNNs alternately stack graph convolutions, linear layers and non-linear activation functions to generate representative representations of nodes. Without loss of generality, the widely used GNNs follow the following form:

$$\mathbf{H}^L = \hat{\mathbf{A}} \sigma \left( \cdots \sigma \left( \hat{\mathbf{A}} \mathbf{X} \mathbf{W} \right) \cdots \right) \mathbf{W}^{L-1} \quad (1)$$

where  $\hat{\mathbf{A}}$  is a weighted matrix for feature propagation,  $\mathbf{W}^l$  is a learnable weight matrix and  $\sigma$  is a non-linear activation function Relu. For example, the GCN [22] utilizes the symmetric normalized adjacent matrix as  $\hat{\mathbf{A}}$ , GraphSAGE [16] utilizes the random walk normalized version, and the GAT [37] applies the attention mechanism [36] to obtain a learnable weighted  $\hat{\mathbf{A}}$ .

**Advanced node interaction GNNs.** Simply stacking graph convolution layers cause the over-smoothing [26] and heterophily [31] problem. Most GNNs equipped residual connections to capture long-range neighbors and alleviate over-smoothing [25, 39]. For instance, the GCNII [8] is the SOTA deep GNN, which extends the GCN with initial connection and identity mapping. There are also works that extend GNNs to heterophilic graphs [1, 27, 31, 48]. Some methods enlarge the receptive field of nodes to include more homophilous

neighbors. H2GCN [48] presents three designs to improve the performance of GNNs under heterophily: ego and neighbor embedding separation, higher-order neighborhood utilization, and intermediate representation combination. Geom-GCN [31] and WRGAT [34] transform the original graph by discovering the non-local semantic similarity neighbor. There also exist GNNs that study graph heterophily by carefully considering local neighbors at each layer. For example, to jointly study the heterophily and over-smoothing problems, GGCN [40] allows propagated signed messages from nodes' local neighbors. It also adopts a degree correction mechanism for node-wise rescaling and further alleviates the over-smoothing problem. FAGCN [4] and ACM-GCN [30] apply both low-pass and high-pass filters in each layer for the neighbor extractor. Despite these advanced GNNs owning high expressiveness, they still suffer from high computational costs and cannot handle large-scale datasets.

**Sampling-based GNNs.** Sampling-based GNNs perform batch training that utilizes sampled subgraphs as a small batch to approximate the full-batch GNNs and reduce memory consumption. There are three categories of widely-used sampling strategies: 1) As a node-wise sampling method, GraphSAGE [16] randomly samples a fixed-size set of neighbors for each node in every layer. VR-GCN [7] further analyzes the variance reduction for node sampling. 2) For layer-wise sampling, Fast-GCN [5] samples a fixed number of nodes at each layer, and ASGCN [19] designs adaptive layer-wise sampling with better variance control. 3) At the graph-level sampling, ClusterGCN [9] first partitions the entire graph into clusters and then samples the nodes in the clusters, and GraphSAINT [43] directly samples a subgraph for mini-batch training. However, these sampling strategies still conduct node interactions that face high communication costs during training, and the model performance is highly sensitive to sampling quality.

**Decoupled GNNs.** Unlike standard GNNs, which sequentially stack non-linear graph convolution layers, decoupled GNNs simplify the graph convolution by decoupling the model into two steps: hop feature propagation and an MLP classifier for prediction. Depending on the propagation order, there are two typical ways to decouple these two operations: (1) *pre-processing* that first pre-computes the feature propagation, *e.g.*,  $\mathbf{X} = \sum_{i=0}^L \theta_i \mathbf{A}^i \mathbf{X}$ , and then applies the MLP classifier for each node representation  $\mathbf{X}^L$  individually. SGC [38] simplifies GNNs into a linear model  $\mathbf{Y} = \mathbf{A}^L \mathbf{X} \mathbf{W}$ , which achieves faster computation. However, it only considers the  $L$  hop features, and the linear layer limits its expressiveness. S2GC [47] extends the SGC by using the simple spectral graph convolution to average the propagated features in multi-hop. It also proposes utilizing MLP as a classifier. Different from S2GC, SIGN [13] uses the concatenation of multi-hop features, with an individual  $\mathbf{W}$  for each hop transformation, to achieve better performance. (2) *post-processing* that propagates multi-hop features after an MLP predictor:  $\mathbf{Y} = \sum_{i=0}^L \theta_i \mathbf{A}^i \text{MLP}(\mathbf{X})$ . To this end, APPNP [23] utilizes the approximate personal PageRank filter as a feature propagator, while GPRGNN [10] further utilizes a learnable generalized PageRank for the weights of theta to enhance performance. However, such post-processing still needs to propagate high-cost features during training, limiting its scalability compared to pre-processing.

Although these decoupled GNNs efficiently propagate features, they usually suffer suboptimal results in heterophilic datasets due to the lack of non-linear interactions among nodes. Similar to pre-processing methods, we also use the pre-computed hop features of nodes for high scalability. The difference lies in that we explicitly consider the non-linear interaction among hops, which is more expressive and can enhance the discriminative ability of nodes.

## 3 METHODOLOGY

### 3.1 HopGNN

As illustrated in Figure 2, our proposed HopGNN framework is composed of four steps, namely, hop preprocessing, hop encoding, hop interaction, hop fusion and prediction. We will introduce them one by one in detail.

**Hop Pre-processing.** Extracting information from long-range neighbors is crucial for nodes to achieve representative representation. Unlike the node interaction GNNs, which stack  $L$  layers to reach  $L$ -hop neighbors and suffer high computational costs with limited scalability [45], our proposed framework is built upon a hop-information pre-processing step. It pre-computes multi-hop node information from the node's original feature vectors and the  $l$ -hop feature can be simplified as:

$$\tilde{\mathbf{X}} = [\mathbf{X}_p; \mathbf{X}_p^1; \dots; \mathbf{X}_p^L], \quad \mathbf{X}_p^l = \hat{\mathbf{A}}^l \mathbf{X} \quad (2)$$

where  $\hat{\mathbf{A}}$  is the normalized adjacent matrix, and  $\tilde{\mathbf{X}}$  contains the multi-hop neighbor information. This pre-processing does not require any learnable parameters and only needs to be computed once in a CPU or distributed system for large-scale graphs. As a result, it can make models naturally support mini-batch training and easily scale to large datasets since it eliminates the computational complexity of node aggregation during training and inference.

**Hop Encoding.** To obtain sufficient expressive power, it is necessary to have at least one learnable linear transformation to transform the input hop features into higher-level hop embedding. For parameter efficiency, we apply a shared parametered linear layer  $f$  to encode all hops. Moreover, unlike previous decoupled GNNs, we add a 1D learnable hop-order encoding vector  $\mathbf{E}_{\text{order}} \in \mathbb{R}^{1 \times L \times d}$  to each node hop embedding to incorporate the order information of the hops.

$$\mathbf{H} = \left[ f(\mathbf{X}_p); f(\mathbf{X}_p^1); \dots; f(\mathbf{X}_p^L) \right] + \mathbf{E}_{\text{order}}. \quad (3)$$

The hop embedding  $\mathbf{H} \in \mathbb{R}^{N \times L \times d}$  contains multi-hop neighbor information. The  $\mathbf{E}_{\text{order}}$  can help the following order-insensitive hop interaction layer to capture hop-order information, which is important for the heterophily datasets, as further discussed in Section 4.3.

**Hop Interaction.** Inspired by [15], we argue that the underlying co-occurrence among different hop features contains the clue for the discrimination of each node. Therefore, our goal is to model the non-linear interaction among hops to enhance discrimination without node interaction. Recall that message-passing is widely used in GNNs to conduct non-linear interactions among nodes [14]. We take advantage of current well-designed GNNs by converting the interaction target from nodes to hop features of each node. Specifically, for each node  $v_i$ , we construct a fully-connected hop feature graph  $\mathcal{G}_i^{\text{hop}} = \{\mathcal{V}^{\text{hop}}, \mathcal{E}^{\text{hop}}\}$ , where each node  $v'_l \in \mathcal{G}_i^{\text{hop}}$  corresponds to an  $l$ -th hop feature of the original node  $v_i$ . Accordingly, the task of

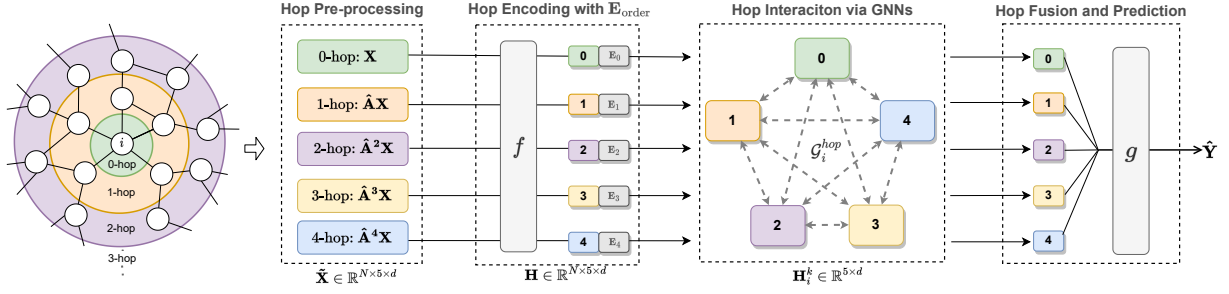


**Figure 2: Overview of the proposed HopGNN framework with four steps, illustration with four hops. The core idea of HopGNN is to convert the target of message-passing from nodes into pre-processed multi-hop features inside each node, which can enhance the nodes’ discriminative power without node interaction.**

modeling hop interactions of node  $v_i$  is equivalent to modeling node interactions on the corresponding hop feature graph, which can be easily achieved by applying any standard GNNs over  $\mathcal{G}_i^{hop}$ . With the residual connection, we can stack  $K$  hop interaction layers to model the high-order interaction among hops, and each layer interaction for node  $v_i$  is:

$$\mathbf{H}_i^k = \text{GNN}(\mathcal{G}_i^{hop}, \mathbf{H}_i^{k-1}) + \mathbf{H}_i^{k-1}, \quad k = 1 \dots K \quad (4)$$

In practice, we do not need to explicitly construct the hop feature graph  $\mathcal{G}^{hop}$  for each node. Instead, for the hop interaction GNN in Eq. (4), without loss of generality, we implement it with a multi-head self-attention mechanism [36, 37] to capture the complex dependencies between hop features, *i.e.*, pairwise interactions between two hop features in different semantic subspaces. For simplicity, we omit the superscript  $k$  and subscript  $i$ , the hop embedding  $\mathbf{H} \in \mathbb{R}^{L \times d}$  of each node is projected by three matrices  $\mathbf{W}_Q$ ,  $\mathbf{W}_K$ , and  $\mathbf{W}_V$  to the corresponding representations  $\mathbf{Q}$ ,  $\mathbf{K}$ , and  $\mathbf{V}$ . The single head of self-attention for each interaction layer is then calculated as:

$$\mathbf{Q} = \mathbf{H}\mathbf{W}_Q, \quad \mathbf{K} = \mathbf{H}\mathbf{W}_K, \quad \mathbf{V} = \mathbf{H}\mathbf{W}_V \quad (5)$$

$$\mathbf{A}' = \text{softmax}\left(\frac{\mathbf{Q}\mathbf{K}^T}{\sqrt{d}}\right), \quad \text{Attn}(\mathbf{H}) = \mathbf{A}'\mathbf{V} \quad (6)$$

where  $\mathbf{A}'$  can be regarded as a weighted feature graph that captures the current interaction strength between pairwise hop features.

Using the above multi-head attention can be regarded as employing GAT over  $\mathcal{G}^{hop}$  to achieve hop interaction. We also compared other GNN architectures to model hop interactions in Section 4.3 and found that they can also achieve comparable performance, which validates the generality and flexibility of our framework.

**Hop Fusion and Prediction.** After hop interaction, we apply a fusion and prediction function  $g$  for each node to generate the final output. We first apply a mean fusion to average all hop representations  $\mathbf{H}^K \in \mathbb{R}^{N \times L \times d}$  into a single representation  $\mathbf{Z} \in \mathbb{R}^{N \times d}$ . Here, we have tested other fusion mechanisms, but we did not observe noticeable improvements. Then, we utilize another simple linear layer with softmax activation for the prediction of downstream tasks.

$$\mathbf{Z} = \text{fusion}(\mathbf{H}^K) \quad (7)$$

$$\hat{\mathbf{Y}} = \text{softmax}(\text{linear}(\mathbf{Z})) \quad (8)$$

The training objective of HopGNN is the standard cross-entropy between the ground truth labels  $\mathbf{Y}$  and the output of the network

$$\hat{\mathbf{Y}} \in \mathbb{R}^{N \times c};$$

$$\mathcal{L}_{ce} = - \sum_{i \in \mathcal{V}_L} \sum_{j=1}^c Y_{ij} \ln \hat{Y}_{ij}. \quad (9)$$

Although training the HopGNN with only  $\mathcal{L}_{ce}$  achieves competitive results, to show the generality and flexibility of our framework, we discuss how to combine HopGNN with recent popular self-supervised objectives [8, 42] in the following section.

### 3.2 Self-Supervised Enhancement

In this subsection, we show that it can easily incorporate the self-supervised learning (SSL) objective to further enhance the performance of HopGNN. Recall that the key idea of HopGNN is to conduct interactions among multi-hops to enhance the discrimination nodes. The desired interaction would help nodes to capture the task-relevant features and drop task-irrelevant features. To encourage such property, recent feature-level SSL studies aim to maximize features’ invariance between two views and minimize the redundancy between dimensions [42, 44]. Formally, in Barlow Twins [42], given the cross-correlation matrix  $\mathbf{C} \in \{-1, 1\}^{d \times d}$  between two views, the SSL objective is:

$$\mathcal{L}_{ssl} \triangleq \underbrace{\sum_i (1 - C_{ii})^2}_{\text{invariance term}} + \underbrace{\alpha \sum_i \sum_{j \neq i} C_{ij}^2}_{\text{redundancy reduction term}} \quad (10)$$

where  $\alpha$  is a scalar to control the decorrelation strength. Inspired by them, we further use multi-task learning to train the HopGNN, with the  $\mathcal{L}_{ce}$  as the main task and  $\mathcal{L}_{ssl}$  as the auxiliary task, and the overall training objective is:

$$\mathcal{L}_{\text{final}} = \mathcal{L}_{ce} + \lambda \mathcal{L}_{ssl}. \quad (11)$$

In our case, as shown in Figure 3, the additional SSL objective is applied after the hop interaction to enhance the representative. To generate two views of hop interaction features, distinguished from the previous works to adopt sophisticated augmentation [8, 29], we simply forward HopGNN twice with different dropout units as augmentations to obtain  $\mathbf{H}^K$  and  $\mathbf{H}'^K$ . Since the training of our model is independent of the graph structure, complex graph-based data augmentation operations are not needed. Then, we not only calculate  $\mathcal{L}_{ce}$  with fusion and prediction steps on both views but also flatten and normalize them to calculate the cross-correlation matrix  $\mathbf{C}$  for  $\mathcal{L}_{ssl}$ . Optimizing such the SSL objective can maximize the

**Table 1: Time and memory complexities.** We consider time complexity for the feature propagation and transformation in the network and memory complexity for storing the activations of node embeddings (we ignore model weights since they are negligible compared to the activations).  $L$  and  $K$  are the number of hops and the non-linear transformation, respectively, and  $d$  is the feature dimension (assumed to be fixed for all layers).  $N$ ,  $|E|$  and  $s$  are the numbers of nodes, edges, and sampling neighborhoods, respectively.  $b$  is the minibatch size.

Category		Method	Minibatch	Pre-Processing Time	Training Time	Training Memory
Standard		GCN/GCNII/...	×	-	$O(LEd + LNd^2)$	$O(LNd)$
Sampling	Node	GraphSAGE	✓	$O(s^L N)$	$O(s^L Nd^2)$	$O(bs^L d)$
	Layer	FastGCN/AS-GCN	✓	-	$O(sLNd^2)$	$O(bsLd)$
	Graph	Cluster-GCN	✓	$O(E)$	$O(LEd + LNd^2)$	$O(bLd)$
	Graph	GraphSAINT	✓	$O(sN)$	$O(LEd + LNd^2)$	$O(bLd)$
Decoupling	Pre	SGC/S2GC	✓	$O(LEd)$	$O(Nd^2)$	$O(bd)$
	Pre	SIGN	✓	$O(LEd)$	$O(KNd^2)$	$O(bLd)$
	Post	APPNP/GPRGNN	×	-	$O(KNd^2 + LEd)$	$O(LNd)$
Hop Interaction		HopGNN	✓	$O(LEd)$	$O(KNd^2 + KNL^2d)$	$O(bLd)$

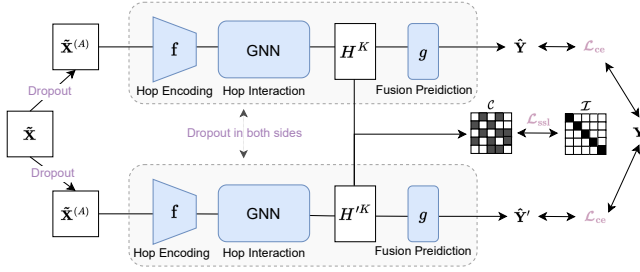


**Figure 3: Multi-task learning with SSL for HopGNN. Illustration inspired by Barlow Twins [42].**

task-relevant mutual information and minimize the task-irrelevant information [44]. It would help the learned hop interaction representation  $H^K$  to extract minimal and sufficient information about downstream tasks from multi-hop neighbors.

Compared with other instance-level contrastive learning paradigms, memory costs of the feature-level  $\mathcal{L}_{ssl}$  do not rise with the graph size since it focuses on the feature dimension, which is scalable and efficient. We provide the result of HopGNN with contrastive learning in the Appendix.

### 3.3 Discussions

**Connection to decoupled GNNs.** From the perspective of hop interaction, the decoupled GNNs learn a fixed linear combination of multi-hop features for all nodes, which is equivalent to applying fixed hop attention coefficients with diagonal parts and remaining off-diagonal as 0. However, such fixed coefficients ignoring the pairwise hop interaction would cause sub-optimal results since each hop’s contribution for different nodes may be different. In contrast, our proposed HopGNN utilizes the self-attention mechanism to learn the representations of different-hop neighbors based on their semantic correlation for each node, which helps the model learn more informative node representations.

**Complexity analysis.** Table 1 provides a detailed asymptotic complexity comparison between HopGNN and other representative GNN methods. 1) The standard node interaction GNNs need full-batch training, and the time complexity contains the feature propagation part  $O(LEd)$  over edges and feature transformation  $O(LNd^2)$  over nodes. Moreover, for memory complexity, we need to store the activation of node embedding in each layer, which has  $O(LNd)$ . Note that we ignore the memory usage of model weights and the optimizer here since they are negligible compared to the activations [12]. The time and memory complexity of full-batch node interaction GNNs are highly correlated to the size of the graphs and result in the scalability problem. 2) Most sampling GNNs reduce the training time and memory cost via mini-batching with the corresponding sampling neighbor size  $s$ . 3) For pre-computed decoupled GNNs, thanks to the pre-processing of feature propagation, the training complexity is the same as the traditional mini-batch training, *e.g.*, MLPs with feature transformation, which is usually smaller than the sampling methods. However, the post-computed decoupled GNNs still require feature propagation during training, leading to a cost similar to that of full-batch GNNs. 4) The computational cost of HopGNN is similar to the pre-computed decoupled GNN, which is also scalable to large-scale graphs. Compared with SIGN, the HopGNN explicitly conducts non-linear interactions among  $L$  hops, which is more expressive and requires  $O(KNL^2d)$  additional time complexity of  $K$  interaction layers.

## 4 EXPERIMENTS

### 4.1 Setup

**Datasets.** We comprehensively evaluate the performance of HopGNN on 12 benchmark datasets. These datasets vary in domain, size and smoothness, including three standard homophily citation datasets [22], six well-known heterophily datasets [31], two large-scale inductive datasets [43] and a large-scale transductive OGB products dataset [18]. For the homophily and heterophily benchmark datasets, we use the same 10 public fixed training/validation/test splits as



**Table 2: Mean test accuracy  $\pm$  stdev on 6 heterophily and 3 homophily real-world datasets over 10 public splits (48%/32%/20% of nodes for training/validation/test). The best performance is highlighted.  $\ddagger$  denotes the results obtained from previous works [40, 48]**

$\mathcal{H}_{\text{edge}}$	Texas	Wisconsin	Actor	Squirrel	Chameleon	Cornell	Citeseer	Pubmed	Cora	Avg
#Nodes	183	251	7,600	5,201	2,277	183	3,327	19,717	2,708	-
#Edges	295	466	26,752	198,493	31,421	280	4,676	44,327	5,278	-
#Classes	5	5	5	5	5	5	7	3	6	-
MLP $\ddagger$	81.89 $\pm$ 4.78	85.29 $\pm$ 3.61	35.76 $\pm$ 0.98	29.68 $\pm$ 1.81	46.36 $\pm$ 2.52	81.08 $\pm$ 6.37	72.41 $\pm$ 2.18	86.65 $\pm$ 0.35	74.75 $\pm$ 2.22	65.99
GCN $\ddagger$	55.14 $\pm$ 5.16	51.76 $\pm$ 3.06	27.32 $\pm$ 1.10	53.43 $\pm$ 2.01	64.82 $\pm$ 2.24	60.54 $\pm$ 5.30	76.50 $\pm$ 1.36	88.42 $\pm$ 0.50	86.90 $\pm$ 1.04	62.76
GAT $\ddagger$	52.14 $\pm$ 5.16	49.41 $\pm$ 4.09	27.44 $\pm$ 0.89	40.72 $\pm$ 1.55	60.26 $\pm$ 2.50	61.89 $\pm$ 5.05	76.55 $\pm$ 1.23	86.33 $\pm$ 0.48	87.30 $\pm$ 1.10	60.23
GraphSAGE $\ddagger$	82.43 $\pm$ 6.14	81.18 $\pm$ 5.56	34.23 $\pm$ 0.99	41.61 $\pm$ 0.74	58.73 $\pm$ 1.68	75.95 $\pm$ 5.01	76.04 $\pm$ 1.30	88.45 $\pm$ 0.50	86.90 $\pm$ 1.04	69.50
GCNII $\ddagger$	77.57 $\pm$ 3.83	80.39 $\pm$ 3.40	37.44 $\pm$ 1.30	38.47 $\pm$ 1.58	63.86 $\pm$ 3.04	77.86 $\pm$ 3.79	77.33 $\pm$ 1.48	90.15 $\pm$ 0.43	88.37 $\pm$ 1.25	70.16
H2GCN-1 $\ddagger$	84.86 $\pm$ 6.77	86.67 $\pm$ 4.69	35.86 $\pm$ 1.03	36.42 $\pm$ 1.89	57.11 $\pm$ 1.58	82.16 $\pm$ 4.80	77.07 $\pm$ 1.64	89.40 $\pm$ 0.34	86.92 $\pm$ 1.37	70.72
H2GCN-2 $\ddagger$	82.16 $\pm$ 5.28	85.88 $\pm$ 4.22	35.62 $\pm$ 1.30	37.90 $\pm$ 2.02	59.39 $\pm$ 1.98	82.16 $\pm$ 6.00	76.88 $\pm$ 1.77	89.59 $\pm$ 0.33	87.81 $\pm$ 1.35	70.87
ACM-GCN $\ddagger$	87.84 $\pm$ 4.40	88.43 $\pm$ 3.22	36.28 $\pm$ 1.09	54.40 $\pm$ 1.88	66.93 $\pm$ 1.85	85.14 $\pm$ 6.07	77.32 $\pm$ 1.70	90.00 $\pm$ 0.52	87.91 $\pm$ 0.95	74.92
WRGAT $\ddagger$	83.62 $\pm$ 5.50	86.98 $\pm$ 3.78	36.53 $\pm$ 0.77	48.85 $\pm$ 0.78	65.24 $\pm$ 0.87	81.62 $\pm$ 3.90	76.81 $\pm$ 1.89	88.52 $\pm$ 0.92	87.95 $\pm$ 1.18	72.90
GGCN $\ddagger$	84.86 $\pm$ 4.55	86.86 $\pm$ 3.29	37.54 $\pm$ 1.56	55.17 $\pm$ 1.58	71.14 $\pm$ 1.84	85.68 $\pm$ 6.63	77.14 $\pm$ 1.45	89.15 $\pm$ 0.37	87.95 $\pm$ 1.05	75.05
S2GC	68.65 $\pm$ 8.05	71.57 $\pm$ 9.01	34.17 $\pm$ 0.92	41.63 $\pm$ 0.98	58.55 $\pm$ 5.15	75.25 $\pm$ 7.82	76.08 $\pm$ 0.45	88.31 $\pm$ 0.38	87.73 $\pm$ 2.90	66.88
SIGN	75.14 $\pm$ 7.94	80.59 $\pm$ 3.75	36.14 $\pm$ 1.01	40.16 $\pm$ 2.12	60.48 $\pm$ 2.10	78.11 $\pm$ 4.67	76.53 $\pm$ 1.76	89.58 $\pm$ 0.45	86.72 $\pm$ 1.37	69.27
APNP	78.37 $\pm$ 6.01	81.42 $\pm$ 4.34	34.64 $\pm$ 1.51	33.51 $\pm$ 2.02	47.50 $\pm$ 1.76	77.02 $\pm$ 7.01	77.06 $\pm$ 1.73	87.94 $\pm$ 0.56	87.71 $\pm$ 1.34	67.24
GPRGNN	82.12 $\pm$ 7.72	81.16 $\pm$ 3.17	33.29 $\pm$ 1.39	43.29 $\pm$ 1.66	61.82 $\pm$ 2.39	81.08 $\pm$ 6.59	75.56 $\pm$ 1.62	86.85 $\pm$ 0.46	86.98 $\pm$ 1.33	70.15
HopGNN	81.35 $\pm$ 4.31	84.96 $\pm$ 4.11	36.66 $\pm$ 1.39	60.95 $\pm$ 1.65	70.13 $\pm$ 1.39	83.70 $\pm$ 6.52	76.16 $\pm$ 1.53	89.98 $\pm$ 0.39	87.12 $\pm$ 1.35	74.56
HopGNN+	82.97 $\pm$ 5.12	85.69 $\pm$ 5.43	37.09 $\pm$ 0.97	64.23 $\pm$ 1.33	71.21 $\pm$ 1.45	84.05 $\pm$ 4.48	76.69 $\pm$ 1.56	90.28 $\pm$ 0.42	87.57 $\pm$ 1.33	75.53

provided in [31]. For large-scale datasets, we use their public splits in [18, 43]. The statistics of these datasets are summarized in Tables 2 and 3. Details on these datasets can be found in the Appendix. **Baselines.** We compare HopGNN with various baselines, including (1) MLP; (2) standard node-interaction GNN methods: GCN [22], GAT [37], GraphSAGE [16] and GCNII [8]; (3) heterophilic GNNs with adaptive node interaction: H2GCN [48], WRGAT [34], ACM-GCN [30], GGCN [40] (4) sampling GNNs: FastGCN [5], AS-GCN [19], ClusterGNN [9], GraphSAINT [43]; and (5) decoupled GNNs: S2GC [47], SIGN [13], APPNP [23], GPRGNN [10]. We report results from previous works with the same experimental setup if available. If the results are not previously reported and codes are provided, we implement them based on the official codes and conduct a hyper-parameter search. We provide more baseline results in the Appendix due to space limits.

**Implementation Details.** Following the standard setting [4, 18], we set the hidden dimension of HopGNN as 128 for the nine small-scale datasets and 256 for the three large-scale datasets. Although tuning the hops and layers usually leads to better results, for simplicity, we fix the number of hops as 6 and the interaction layer as 2 of HopGNNs for all datasets in Table 2 and 3. We use Adam [21] for optimization and LayerNorm [3] of each layer and tune the other hyper-parameters. Details can be found in the Appendix.

## 4.2 Overall Performance

**Results on Homophily and Heterophily.** From Table 2, we make the following observations: 1) Standard node interactions are sometimes inferior to MLP, such as Actor and Cornell, indicating that simply stacking node interaction may fail in the heterophily datasets.

**Table 3: Comparison over a large-scale dataset.  $\ddagger$  denotes the results obtained from previous works [41].**

Type	Flickr	Reddit	Products
#Nodes	Inductive	Inductive	Transductive
#Edges	89,250	232,965	2,449,029
#Classes	899,756	11,606,919	61,859,140
	7	41	47
GCN $\ddagger$	49.2 $\pm$ 0.3	93.3 $\pm$ 0	75.64 $\pm$ 0.21
SGC $\ddagger$	50.2 $\pm$ 0.1	94.9 $\pm$ 0	74.87 $\pm$ 0.25
SIGN $\ddagger$	51.4 $\pm$ 0.1	96.8 $\pm$ 0	77.60 $\pm$ 0.13
S2GC	50.48 $\pm$ 0.07	94.04 $\pm$ 0.03	76.84 $\pm$ 0.20
GraphSAGE $\ddagger$	50.1 $\pm$ 1.3	95.3 $\pm$ 0.1	78.29 $\pm$ 0.16
FastGCN $\ddagger$	50.4 $\pm$ 0.1	92.4 $\pm$ 0.1	73.46 $\pm$ 0.20
AS-GCN $\ddagger$	50.4 $\pm$ 0.2	96.4 $\pm$ 0.1	-
ClusterGCN $\ddagger$	48.1 $\pm$ 0.5	95.4 $\pm$ 0.1	78.97 $\pm$ 0.33
GraphSAINT $\ddagger$	51.1 $\pm$ 0.1	96.6 $\pm$ 0.1	79.08 $\pm$ 0.24
HopGNN	52.49 $\pm$ 0.15	96.92 $\pm$ 0.05	79.96 $\pm$ 0.11
HopGNN+	52.68 $\pm$ 0.16	96.98 $\pm$ 0.04	80.08 $\pm$ 0.08

However, the heterophilic GNNs achieve better performance in general, *e.g.*, their average performance over nine datasets is all larger than 70. The reason is that such advanced node interaction can adaptively consider the influence of neighbors in each hop. 2) Compared with heterophilic GNNs, decoupled GNNs achieve sub-optimal results, *i.e.*, their overall performance is less than 70, due to missing the non-linear interaction among nodes. 3) HopGNN achieves

**Table 4: Ablation studies on order embedding, fusion and interaction types for heterophily and homophily graphs.**

		Heterophily	Homophily
HopGNN		69.63	84.42
w/o $E_{\text{order}}$		60.93 $\downarrow 8.70$	83.96 $\downarrow 0.46$
Fusion	Attention	69.81 $\uparrow 0.18$	84.60 $\uparrow 0.18$
	Max	69.50 $\downarrow 0.13$	84.39 $\downarrow 0.03$
Interaction	None	65.59 $\downarrow 4.04$	84.35 $\downarrow 0.07$
	MLP	67.21 $\downarrow 2.42$	84.41 $\downarrow 0.01$
	GCN	68.18 $\downarrow 1.45$	84.38 $\downarrow 0.04$
	SAGE	69.11 $\downarrow 0.52$	84.45 $\uparrow 0.03$

significantly better performance than decouple GNN and is comparable with the SOTA heterophilic GNNs. Such results show that even without complex node interactions, the non-linear interaction among hops can enhance node discrimination in both homophily and heterophily. This validates the effectiveness and generality of the hop interaction paradigm. (4) Moreover, combining the SSL, the HopGNN+ consistently outperforms HopGNN and achieves the best overall performance, validating the effectiveness of the multi-task learning strategy and the compatibility of HopGNN.

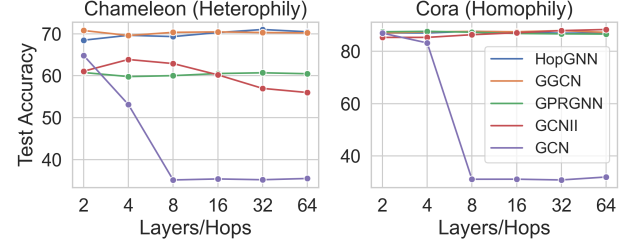
**Results on Large-scale Datasets.** We compare the HopGNN with scalable GNNs, including pre-processing decoupled GNNs and sampling-based GNNs in Table 3, and find that: 1) The decoupled SIGN performs better in the inductive setting, and the subgraph-based GraphSAINT outperforms other baselines in the large-scale transductive product dataset. 2) HopGNN consistently outperforms all the baseline methods in these large-scale datasets. The results in the inductive setting of Flickr and Reddit substantiate the ability of HopGNN to generalize to unseen nodes. Moreover, the HopGNN+ combined feature-level SSL objective still works well in large-scale scenarios and achieves better performance.

### 4.3 Ablation Study

In this part, we study the role of the hop-order embedding  $E_{\text{order}}$ , hop interaction and hop fusion type to validate the effectiveness of each component and the generality of the whole framework. Due to space limits, we report the average test accuracy of these variants across three homophilic and six heterophilic datasets, as shown in Table 4.

**Hop-order embedding.** Without hop-order embedding, the performance drops slightly in homophily (0.46) but dramatically in heterophily (8.7). This indicates that hop-order information is more crucial for order-insensitive hop interactions in challenging heterophilic scenarios. The reason may be that the contribution varies in different order hop of neighbors, which is also discussed in H2GNN [48] that high-order neighbors are expected to be homophily dominant and useful for heterophilic datasets.

**Hop fusion.** We also test the effects of max- and attention-based fusion mechanisms in HopGNN and observe their similar performance under both heterophily and homophily. Although the attention-based fusion achieves slightly higher results, we still choose the mean fusion as the default due to its simplicity and efficiency.

**Figure 4: Classification accuracy with different layers/hops.**

**Hop interaction.** For the hop interaction layer, we test the variant of no interaction, interaction with GCN and SAGE, and interaction with MLP. We make the following observations: 1) They perform closely under homophily since the nodes' neighbors share similar information, resulting in limited gain from interactions. 2) Removing the interaction incurs a performance reduction of 4.04 in heterophily datasets, and the interaction based on MLP also results in a 2.3 performance drop. These results are consistent with the limited performance of decoupled GNNs using linear combination or concatenation among hops. Such performance degeneration further validates the importance of hop-level interaction since it can investigate discriminative clues of nodes for the classification in heterophily. 3) For the interaction of GNN variants, both standard GCN and SAGE achieve competitive results, demonstrating that our framework is stable with different GNN-based hop interaction mechanisms. We choose the multi-head attention mechanism in GAT as the default due to its generalizability.

### 4.4 In-depth Analysis

**Over-smoothing.** To test the robustness of the models to over-smoothing, we compared the HopGNN with the classical GCN and different kinds of SOTA, including GRPGNN from decoupled GNNs, GCNII from deep GNNs, and GCNN from heterophilic GNNs. From Figure 4, we have the following observations: 1) The performance of the GCN drops rapidly as the number of layers increases. However, all the other models do not suffer over-smoothing in the homophilic datasets. 2) Both GCNII and GPRGNN significantly underperform the GGCN and HopGNN under all layers in Chameleon. This means that although decoupling and residual connection can solve the over-smoothing to some extent, they are insufficient for heterophily. 3) The GGCN conducts adaptive node interactions in each layer by carefully considering each hop neighbor's information, which is expressive but limits its scalability. Notably, without node interaction, the HopGNN still achieves robustness under different layers in both homophily and heterophily, validating the superiority of the hop interaction paradigm.

**Efficiency.** In Figure 5, we fairly evaluate the throughputs and actual memory of various representative methods, i.e., the best model of each kind in the large-scale products dataset, under different layers during the training procedure. The implementation details can be found in the Appendix. We observe that: 1) The basic GraphSAGE is significantly slower and costs a huge amount of memory due to the neighbor explosion. Sub-graph sampling makes GraphSAINT

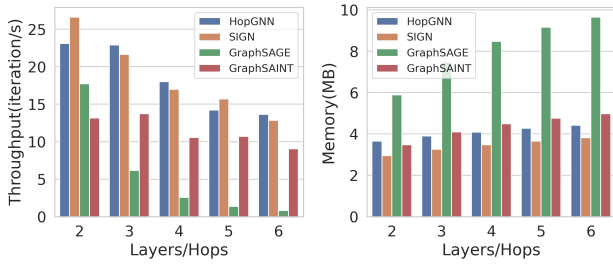


**Figure 5: The comparison of throughput (left) and memory usage (right) in the Products dataset, both are shown in the log scale for better illustration.**

significantly reduce time and memory costs. 2) The decoupled SIGN achieves faster and smaller memory cost than GraphSAINT, but with sub-optimal results as shown in Table 3. 3) HopGNN costs slightly more memory than SIGN due to the additional hop interaction phase, but HopGNN achieves the best performance and is faster than GraphSAINT, which indicates a better trade-off between performance and scalability. These results meet the complex analysis in Section 3.3.

## 5 CONCLUSION

We have presented a novel hop interaction paradigm, a practical solution to address the scalability and over-smoothing problem of GNNs simultaneously. Specifically, we design a simple yet effective HopGNN framework. It first pre-computes non-parameter aggregation of multi-hop features only once to reduce the computational cost during training and inference. Then, it conducts non-linear interaction among the multi-hop features of each node to enhance their discriminative abilities. We also develop a multi-task learning strategy with the self-supervised objective to enhance the performance of the downstream task. Experiments on 12 benchmark datasets show that HopGNN achieves state-of-the-art performance while maintaining high scalability and efficiency. One future work is to investigate advanced interaction mechanisms among hops to enhance the performance of HopGNNs. It is also interesting to apply the HopGNN to other downstream tasks, such as graph classification and link prediction.

## REFERENCES

- [1] Sami Abu-El-Haija, Bryan Perozzi, Amol Kapoor, Nazanin Alipourfard, Kristina Lerman, Hrayr Harutyunyan, Greg Ver Steeg, and Aram Galstyan. 2019. Mix-hop: Higher-order graph convolutional architectures via sparsified neighborhood mixing. In *International Conference on Machine Learning*. PMLR, 21–29.
- [2] Uri Alon and Eran Yahav. 2020. On the Bottleneck of Graph Neural Networks and its Practical Implications. In *International Conference on Learning Representations*.
- [3] Jimmy Ba, Jamie Ryan Kiros, and Geoffrey E. Hinton. 2016. Layer normalization. *preprint arXiv:1607.06450* (2016).
- [4] Deyu Bo, Xiao Wang, Chuan Shi, and Huawei Shen. 2021. Beyond low-frequency information in graph convolutional networks. In *Proceedings of the AAAI Conference on Artificial Intelligence*, Vol. 35. 3950–3957.
- [5] Jie Chen, Tengfei Ma, and Cao Xiao. 2018. FastGCN: Fast learning with graph convolutional networks via importance sampling. In *6th International Conference on Learning Representations, ICLR 2018, Vancouver, BC, Canada, April 30 - May 3, 2018. Conference Track Proceedings*. OpenReview.net.
- [6] Jianfei Chen, Lianmin Zheng, Zhewei Yao, Dequan Wang, Ion Stoica, Michael W Mahoney, and Joseph E Gonzalez. 2021. ActNN: Reducing Training Memory Footprint via 2-Bit Activation Compressed Training. In *International Conference on Machine Learning*.
- [7] Jianfei Chen, Jun Zhu, and Le Song. 2018. Stochastic Training of Graph Convolutional Networks with Variance Reduction. In *International Conference on Machine Learning*. PMLR, 942–950.
- [8] Ming Chen, Zhewei Wei, Zengfeng Huang, Bolin Ding, and Yaliang Li. 2020. Simple and deep graph convolutional networks. In *International Conference on Machine Learning*. PMLR, 1725–1735.
- [9] Wei-Lin Chiang, Xuanqing Liu, Si Si, Yang Li, Samy Bengio, and Cho-Jui Hsieh. 2019. Cluster-gcn: An efficient algorithm for training deep and large graph convolutional networks. In *Proceedings of the 25th ACM SIGKDD International Conference on Knowledge Discovery & Data Mining*. 257–266.
- [10] Eli Chien, Jianhao Peng, Pan Li, and Olga Milenkovic. 2021. Adaptive universal generalized pageRank graph neural network. In *International Conference on Learning Representations*.
- [11] Michaël Defferrard, Xavier Bresson, and Pierre Vandergheynst. 2016. Convolutional neural networks on graphs with fast localized spectral filtering. *Advances in neural information processing systems* 29 (2016).
- [12] Keyu Duan, Zirui Liu, Peihao Wang, Wenqing Zheng, Kaixiong Zhou, Tianlong Chen, Xia Hu, and Zhangyang Wang. 2022. A Comprehensive Study on Large-Scale Graph Training: Benchmarking and Rethinking. *preprint arXiv:2210.07494* (2022).
- [13] Fabrizio Frasca, Emanuele Rossi, Davide Eynard, Ben Chamberlain, Michael Bronstein, and Federico Monti. 2020. Sign: Scalable inception graph neural networks. *preprint arXiv:2004.11198* (2020).
- [14] Justin Gilmer, Samuel S Schoenholz, Patrick F Riley, Oriol Vinyals, and George E Dahl. 2017. Neural message passing for quantum chemistry. In *International Conference on Machine Learning*. JMLR.org, 1263–1272.
- [15] Huifeng Guo, Ruiming Tang, Yunming Ye, Zhenguo Li, and Xiuqiang He. 2017. DeepFM: A Factorization-Machine based Neural Network for CTR Prediction. In *IJCAI*.
- [16] William L Hamilton, Rex Ying, and Jure Leskovec. 2017. Inductive representation learning on large graphs. In *Advances in Neural Information Processing Systems*. 1025–1035.
- [17] Xiangnan He, Kuan Deng, Xiang Wang, Yan Li, Yongdong Zhang, and Meng Wang. 2020. Lightgcn: Simplifying and powering graph convolution network for recommendation. In *Proceedings of the 43rd International ACM SIGIR conference on research and development in Information Retrieval*. 639–648.
- [18] Weihua Hu, Matthias Fey, Marinka Zitnik, Yuxiao Dong, Hongyu Ren, Bowen Liu, Michele Catasta, and Jure Leskovec. 2020. Open graph benchmark: Datasets for machine learning on graphs. In *Advances in Neural Information Processing Systems 33: Annual Conference on Neural Information Processing Systems 2020, NeurIPS 2020, December 6-12, 2020, virtual*.
- [19] Wenbin Huang, Tong Zhang, Yu Rong, and Junzhou Huang. 2018. Adaptive sampling towards fast graph representation learning. *Advances in neural information processing systems* 31 (2018).
- [20] Prannay Khosla, Piotr Teterwak, Chen Wang, Aaron Sarna, Yonglong Tian, Phillip Isola, Aaron Maschinot, Ce Liu, and Dilip Krishnan. 2020. Supervised contrastive learning. *Advances in Neural Information Processing Systems* 33 (2020), 18661–18673.
- [21] Diederik P Kingma and Jimmy Ba. 2014. Adam: A method for stochastic optimization. *preprint arXiv:1412.6980* (2014).
- [22] Thomas N. Kipf and Max Welling. 2017. Semi-supervised classification with graph convolutional networks. In *International Conference on Learning Representations*.
- [23] Johannes Klicpera, Aleksandar Bojchevski, and Stephan Günnemann. 2019. Predict then propagate: Graph neural networks meet personalized pagerank. In *International Conference on Learning Representations*.
- [24] Guohao Li, Matthias Müller, Guocheng Qian, Itzel Carolina Delgadillo Perez, Abdulallah Abualshour, Ali Kassem Thabet, and Bernard Ghanem. 2021. DeepGCNs: Making GCNs go as deep as CNNs. *IEEE Transactions on Pattern Analysis and Machine Intelligence* (2021).
- [25] Guohao Li, Matthias Müller, Ali K. Thabet, and Bernard Ghanem. 2019. DeepGCNs: Can GCNs go as deep as CNNs?. In *2019 IEEE/CVF International Conference on Computer Vision, ICCV 2019, Seoul, Korea (South), October 27 - November 2, 2019*. IEEE, 9266–9275. <https://doi.org/10.1109/ICCV.2019.00936>
- [26] Qimai Li, Zhichao Han, and Xiao-Ming Wu. 2018. Deeper insights into graph convolutional networks for semi-supervised learning. In *Proceedings of the AAAI Conference on Artificial Intelligence*, Vol. 33. 3538–3545.
- [27] Xiang Li, Renyu Zhu, Yao Cheng, Caihua Shan, Siqiang Luo, Dongsheng Li, and Weining Qian. 2022. Finding Global Homophily in Graph Neural Networks When Meeting Heterophily. *preprint arXiv:2205.07308* (2022).
- [28] Meng Liu, Hongyang Gao, and Shuiwang Ji. 2020. Towards deeper graph neural networks. In *Proceedings of the 26th ACM SIGKDD International Conference on Knowledge Discovery & Data Mining*. 338–348.
- [29] Yixin Liu, Ming Jin, Shirui Pan, Chuan Zhou, Yu Zheng, Feng Xia, and Philip Yu. 2022. Graph self-supervised learning: A survey. *IEEE Transactions on Knowledge and Data Engineering* (2022).



- [30] Sitao Luan, Chenqing Hua, Qincheng Lu, Jiaqi Zhu, Mingde Zhao, Shuyuan Zhang, Xiao-Wen Chang, and Doina Precup. 2021. Is Heterophily A Real Nightmare For Graph Neural Networks To Do Node Classification? *preprint arXiv:2109.05641* (2021).
- [31] Hongbin Pei, Bingzhe Wei, Kevin Chen-Chuan Chang, Yu Lei, and Bo Yang. 2020. Geom-GCN: Geometric graph convolutional networks. In *International Conference on Learning Representations*.
- [32] Weijing Shi and Raj Rajkumar. 2020. Point-gnn: Graph neural network for 3d object detection in a point cloud. In *Proceedings of the IEEE/CVF conference on computer vision and pattern recognition*. 1711–1719.
- [33] Jianhua Sun, Qinhong Jiang, and Cewu Lu. 2020. Recursive Social Behavior Graph for Trajectory Prediction. In *Proceedings of the IEEE/CVF Conference on Computer Vision and Pattern Recognition (CVPR)*.
- [34] Susheel Suresh, Vinith Budde, Jennifer Neville, Pan Li, and Jianzhu Ma. 2021. Breaking the Limit of Graph Neural Networks by Improving the Assortativity of Graphs with Local Mixing Patterns. In *KDD*. 1541–1551.
- [35] Laurens Van der Maaten and Geoffrey Hinton. 2008. Visualizing data using t-SNE. *Journal of machine learning research* 9, 11 (2008).
- [36] Ashish Vaswani, Noam Shazeer, Niki Parmar, Jakob Uszkoreit, Llion Jones, Aidan N Gomez, Łukasz Kaiser, and Illia Polosukhin. 2017. Attention is all you need. In *Advances in Neural Information Processing Systems*. 5998–6008.
- [37] Petar Veličković, Guillem Cucurull, Arantxa Casanova, Adriana Romero, Pietro Liò, and Yoshua Bengio. 2018. Graph Attention Networks. In *International Conference on Learning Representations*.
- [38] Felix Wu, Amauri Souza, Tianyi Zhang, Christopher Fifty, Tao Yu, and Kilian Weinberger. 2019. Simplifying graph convolutional networks. In *International Conference on Machine Learning*. PMLR, 6861–6871.
- [39] Keyulu Xu, Chengtao Li, Yonglong Tian, Tomohiro Sonobe, Ken-ichi Kawarabayashi, and Stefanie Jegelka. 2018. Representation learning on graphs with jumping knowledge networks. In *International Conference on Machine Learning*. PMLR, 5453–5462.
- [40] Yujun Yan, Milad Hashemi, Kevin Swersky, Yaoqing Yang, and Danai Koutra. 2021. Two sides of the same coin: heterophily and oversmoothing in graph convolutional neural networks. *preprint arXiv:2102.06462* (2021).
- [41] Jiaxuan You, Zitao Ying, and Jure Leskovec. 2020. Design space for graph neural networks. *Advances in Neural Information Processing Systems* 33 (2020), 17009–17021.
- [42] Jure Zbontar, Li Jing, Ishan Misra, Yann LeCun, and Stéphane Deny. 2021. Barlow twins: Self-supervised learning via redundancy reduction. In *International Conference on Machine Learning*. PMLR, 12310–12320.
- [43] Hanqing Zeng, Hongkuan Zhou, Ajitesh Srivastava, Rajgopal Kannan, and Viktor K. Prasanna. 2020. GraphSAINT: Graph sampling based inductive learning method. In *8th International Conference on Learning Representations, ICLR 2020, Addis Ababa, Ethiopia, April 26–30, 2020*. OpenReview.net.
- [44] Hengrui Zhang, Qitian Wu, Junchi Yan, David Wipf, and Philip S Yu. 2021. From canonical correlation analysis to self-supervised graph neural networks. *Advances in Neural Information Processing Systems* 34 (2021), 76–89.
- [45] Shichang Zhang, Yozen Liu, Yizhou Sun, and Neil Shah. 2022. Graph-less Neural Networks: Teaching Old MLPs New Tricks Via Distillation. In *International Conference on Learning Representations*.
- [46] Yifan Zhang, Bryan Hooi, Dapeng Hu, Jian Liang, and Jiashi Feng. 2021. Unleashing the power of contrastive self-supervised visual models via contrast-regularized fine-tuning. *Advances in Neural Information Processing Systems* 34 (2021), 29848–29860.
- [47] Hao Zhu and Piotr Koniusz. 2020. Simple spectral graph convolution. In *International Conference on Learning Representations*.
- [48] Jiong Zhu, Yujun Yan, Lingxiao Zhao, Mark Heimann, Leman Akoglu, and Danai Koutra. 2020. Beyond homophily in graph neural networks: Current limitations and effective designs. In *Advances in Neural Information Processing Systems*, Vol. 33.

## A APPENDIX

### A.1 Details of Datasets

We provide the details of the three homophily datasets, six heterophily datasets and three large-scale datasets in the following:

- Homophily Datasets
  - *Citeseer*, *Pubmed*, *Cora* [22]: For the benchmark citation datasets, nodes correspond to papers, edges correspond to citation links, the sparse bag-of-words are the features, and each node’s label represents the paper’s topic.
- Heterophily Datasets

- *Texas*, *Wisconsin*, *Cornell* [31]: Nodes and edges represent the web pages and hyperlinks captured from the computer science departments of these universities in the WebKB dataset. Nodes’ features are bag-of-word representations of contents on these web pages. Each node is labeled into five categories: student, project, course, staff, and faculty.
- *Squirrel*, *Chameleon* [31]: Chameleon and Squirrel are web pages extracted from different topics in Wikipedia. Nodes and edges denote the web pages and hyperlinks among them, respectively, and informative nouns in the web pages are employed to construct the node features in the bag-of-word form. Webpages are labeled in terms of the average monthly traffic level.
- *Actor* [31]: The actor network contains the co-occurrences of actors in films, which describes the complex relationships among films, directors, actors and writers. In this network, nodes and edges represent actors and their co-occurrences in films, respectively. The actor’s Wikipedia page is used to extract features and node labels.

- Large-scale Datasets

- *Flickr*, *Reddit* [16, 43]: Flickr and Reddit are inductive datasets for multiclass categorization. The goal of Reddit is to predict online post communities based on user comments. The task of Flickr is to classify the categories of images based on their description and common characteristics of online photographs.
- *Products* [18]: The Products dataset is a large-scale Amazon product co-purchasing network in a transductive setting. Nodes represent products sold in Amazon, edges indicate the products purchased together, and features are 100-dimensional product descriptions after Principal Component Analysis. Labels are the category of products.

### A.2 Implementation Details

**Hyper-parameters.** For HopGNN, we search the hyper-parameters, including learning rate from [0.01, 0.001, 0.005], weight decay from [0, 5e-4, 5e-5, 5e-6], dropout rate from [0.2, 0.4, 0.5, 0.6],  $\alpha$  from [0.01, 0.1, 0.5, 0.8] and  $\lambda$  from [1e-4, 5e-4] via validation sets of each dataset. For other baselines, we search the layers/hops from [2, 8, 16, 32] and fix the hidden dimensions as 128. The search space of other hyper-parameters, such as learning rate, weight decay, and dropout, is the same as that of HopGNN.

**Hardware and Environment.** We run our experiments on a single machine with Intel Xeon CPUs (Gold 5120 @ 2.20GHz), one NVIDIA Tesla V100 GPU (32GB of memory) and 512GB DDR4 memory. We use PyTorch 1.11.0 with CUDA 10.2 to train the model on GPUs.

**Throughput and Memory.** For fairness, we set the hidden dimension to 256 and control the batchsize as 3000 across different models on the Products dataset. We report the hardware throughput and activation usage-based on [6, 12]. The throughput measures how many times each model can complete training steps within a second. We measure the activation memory using `torch.cuda.memory_allocated`.

**Table 5: Mean test accuracy  $\pm$  stdev. The best performance is highlighted.  $\ddagger$  denotes the results obtained from previous works [40, 48].**

	Texas	Wisconsin	Actor	Squirrel	Chameleon	Cornell	Citeseer	Pubmed	Cora	Avg
GCN+JK $\ddagger$	66.49 $\pm$ 6.64	74.31 $\pm$ 6.43	34.18 $\pm$ 0.85	40.45 $\pm$ 1.61	63.42 $\pm$ 2.00	64.59 $\pm$ 8.68	74.51 $\pm$ 1.75	88.41 $\pm$ 0.45	86.79 $\pm$ 0.92	65.79
GCN-Cheby $\ddagger$	77.30 $\pm$ 4.07	79.41 $\pm$ 4.46	34.11 $\pm$ 1.09	43.86 $\pm$ 1.64	55.24 $\pm$ 2.76	74.32 $\pm$ 7.46	75.82 $\pm$ 1.53	88.72 $\pm$ 0.55	86.76 $\pm$ 0.95	68.39
MixHop $\ddagger$	77.84 $\pm$ 7.73	75.88 $\pm$ 4.90	32.22 $\pm$ 2.34	43.80 $\pm$ 1.48	60.50 $\pm$ 2.53	73.51 $\pm$ 6.34	76.26 $\pm$ 1.33	85.31 $\pm$ 0.61	87.61 $\pm$ 0.85	68.21
GEOM $\ddagger$	67.57	64.12	31.63	38.14	60.90	60.81	77.99	90.05	85.27	64.05
FAGCN	78.11 $\pm$ 5.01	81.56 $\pm$ 4.64	35.41 $\pm$ 1.18	42.43 $\pm$ 2.11	56.31 $\pm$ 3.22	76.12 $\pm$ 7.65	74.86 $\pm$ 2.42	85.74 $\pm$ 0.36	83.21 $\pm$ 2.04	68.18
DAGNN	70.27 $\pm$ 4.93	71.76 $\pm$ 5.25	35.51 $\pm$ 1.10	30.29 $\pm$ 2.23	45.92 $\pm$ 2.30	73.51 $\pm$ 7.18	76.44 $\pm$ 1.97	89.37 $\pm$ 0.52	86.82 $\pm$ 1.67	64.43
HopGNN	81.35 $\pm$ 4.31	84.96 $\pm$ 4.11	36.66 $\pm$ 1.39	60.95 $\pm$ 1.65	70.13 $\pm$ 1.39	83.70 $\pm$ 6.52	76.16 $\pm$ 1.53	89.98 $\pm$ 0.39	87.12 $\pm$ 1.35	74.56
HopGNN+	82.97 $\pm$ 5.12	85.69 $\pm$ 5.43	37.09 $\pm$ 0.97	64.23 $\pm$ 1.33	71.21 $\pm$ 1.45	84.05 $\pm$ 4.48	76.69 $\pm$ 1.56	90.28 $\pm$ 0.42	87.57 $\pm$ 1.33	75.53
HopGNN+SCL	81.65 $\pm$ 7.47	84.37 $\pm$ 4.91	36.72 $\pm$ 1.05	61.42 $\pm$ 1.98	70.45 $\pm$ 1.03	84.32 $\pm$ 6.71	76.59 $\pm$ 1.51	90.01 $\pm$ 0.29	87.28 $\pm$ 1.71	74.76

### A.3 More Experiment Results

**More Baselines.** We provide more baseline results in Table 5, including 1) the classical advanced node interaction with high-order neighbor information: GCN+JK [39], GCN-ChebyNet [11], and MixHop [1]. 2) the heterophilic GNNs: Geom-GCN [31] and FAGCN [4] and 3) decoupled GNN: DAGNN [28]. However, their average performance on nine datasets is less than 70, indicating that they have been shown to be outperformed by the state-of-the-art methods.

**Supervised Contrastive Learning Objective.** As discussed in [46], the supervised contrastive loss [20] (SCL) may help to regularize the feature space and make it more discriminative, *i.e.*, minimizing the SCL is equivalent to minimizing the class-conditional entropy  $\mathcal{H}(\mathbf{H}|\mathbf{Y})$  and maximizing the feature entropy  $\mathcal{H}(\mathbf{H})$ . Therefore, it can also be used to enhance the discriminative ability of hop interaction, and we provide the results of HopGNN with SCL in Table 5. Formally, the SCL objective can be defined as:

$$\mathcal{L}_{\text{final}} = \mathcal{L}_{\text{CE}} + \lambda \mathcal{L}_{\text{SCL}}, \quad (12)$$

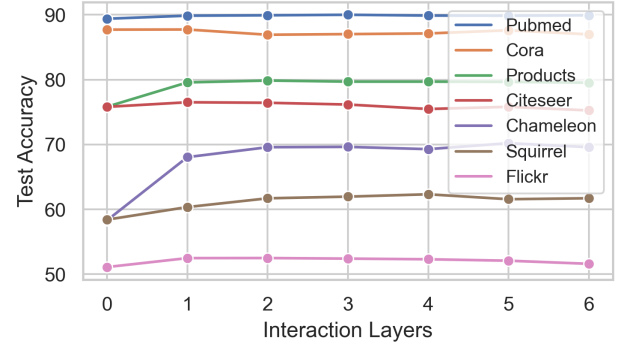
$$\mathcal{L}_{\text{SCL}} = \sum_{i \in I_{\mathcal{L}}} \frac{-1}{|P(i)|} \sum_{p \in P(i)} \log \frac{\exp(\mathbf{h}_i \cdot \mathbf{h}_p / \tau)}{\sum_{a \in A(i)} \exp(\mathbf{h}_i \cdot \mathbf{h}_a / \tau)}, \quad (13)$$

where  $i \in I_{\mathcal{L}} \equiv \{1 \dots 2b\}$  is the index of an arbitrary augmented sample within a training batch (size= $b$ ), and  $A(i) \equiv I_{\mathcal{L}} \setminus \{i\}$ .  $P(i) \equiv \{p \in A(i) : \mathbf{y}_p = \mathbf{y}_i\}$  is the set of indices of all positives that share same label  $y$  in a multiview batch distinct from  $i$ , and  $|P(i)|$  is its cardinality.

As shown in the last row of Table 5, the result demonstrates that the SCL can also improve the performance of HopGNN and is comparable with HopGNN+, which validates the compatibility of the HopGNN framework to different SSL objectives. However, the complexity of SCL is  $O(N^2)$  in a batch due to the instance discrimination task. Therefore, the SCL is not as scalable as the feature-level SSL used in HopGNN+.

**The Effects of Interaction Layers.** We test the effects of different interaction layers in HopGNN under various datasets, including Cora, Citeseer, and Pubmed as homophily examples; Chameleon and Squirrel as heterophily examples; Flickr and Products as large-scale examples. In Figure 6, we observe that HopGNN achieves competitive results using two interaction layers in most cases. Thus, we adopt the default layers of hop interaction as two. Compared with homophily datasets, increasing the layers of hop interaction

would remarkably boost the performance of heterophily datasets. The reason may be that such high-order hop interactions may capture the co-occurrence pattern of multi-hop neighbors, which contain the discriminative clues for heterophily.

**Figure 6: Classification accuracy with different interaction layers.**

**Visualization of Representation.** To qualitatively investigate the effectiveness of the learned feature representation of nodes, we provide a visualization of the t-SNE [35] for the last layer features of GCN (node interaction), SIGN (decoupled), and HopGNN (hop interaction) on the Chameleon (Figure 7) and Cora (Figure 8). Compared with GCN (first row), the SIGN (second row) and HopGNN (last row) are both robust when increasing layers under the Chameleon and Cora. Moreover, the representation of HopGNN exhibits more discernible clustering in Chameleon. Note that these clusters correspond to the five classes of the dataset, verifying the better discriminative power of HopGNN under different layers in Heterophily.

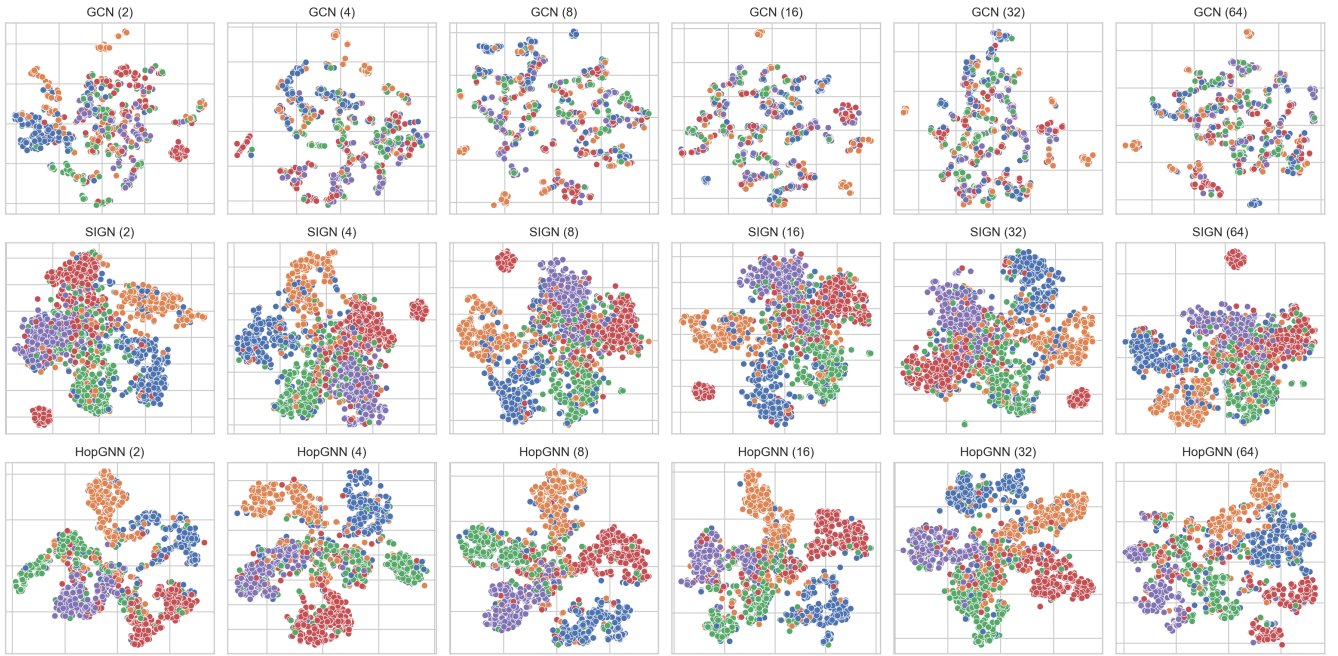


**Figure 7: t-SNE visualization of node representations derived by different numbers of layers/hops of models on Chameleon. Colors represent node classes, and the number in the bracket indicates the layers/hops. Note that these clusters correspond to the five classes, indicating that HopGNN has better discriminative power under different layers in heterophily.**

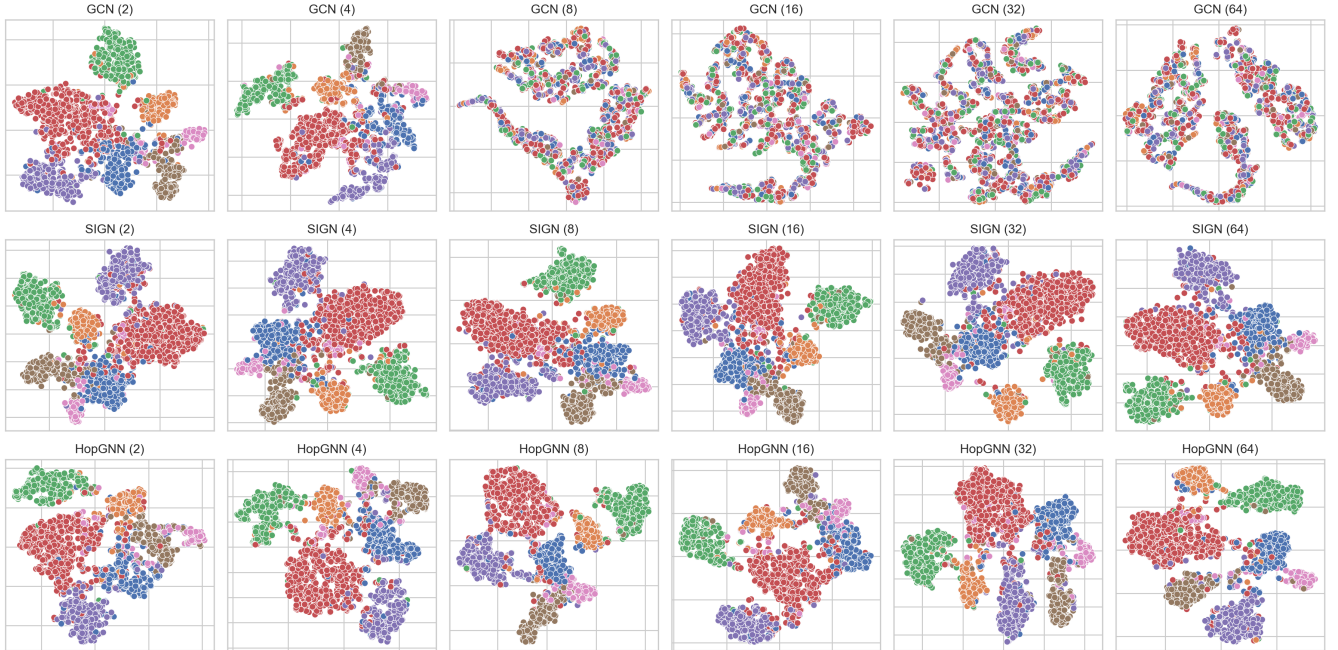


**Figure 8: t-SNE visualization of node representations derived by different numbers of layers/hops of models on Cora. Compared with GCN, the representation of both SIGN and HopGNN are discriminative when increasing layers in a homophily scenario. However, due to the simplicity of homophily datasets, the SIGN and HopGNN achieve similar results.**